Evolution of Accreting Young Massive Objects

National Aeronautics and Space Administration

Harold W. Yorke

Jet Propulsion Laboratory, California Institute of Technology, 4800 Oak Grove Drive, Pasadena, CA 91109

ABSTRACT: Young stars and protostars gain much if not most of their mass via accretion through an accretion disk, starting with a low mass object (a few Jupiter masses) in hydrostatic equilibrium and gradually growing in mass as they accrete material. The time scale for this process is relatively short, typically less than several 10^5 yr, implying mass accretion rates in excess of 10^{-4} $M_\odot$ yr^{-1} for stars of 10 $M_\odot$ and higher. Evolutionary tracks of accreting protostars are calculated and compared to those of non-accreting protostars. "Bloating" of stellar radii well in excess of 100 $R_\odot$ is possible after about 5 $M_\odot$ have accreted; prior to the bloating the stellar radius is several $R_\odot$. We find that the accretion luminosity of accreting protostars dominates during early phases (low stellar masses but with a small radius). The stellar luminosity dominates during the late accretion phases. Molecular core collapse case "F" (10 $M_\odot$) discussed by Yorke & Bodenheimer (1999) is recalculated using a modified version of the original 2D radiation-hydro code: Material flowing into the central zone is added to a spherically symmetric hydrostatic object whose evolution is simultaneously followed using a stellar evolution code.

Introduction: Why do these Calculations?

- Disks are intimately involved in the accretion and growth of protostellar mass during early collapse phases.
- Accretion onto the surface of relatively compact (proto-)stellar objects (whether hydrogen-burning or "pre-main sequence") strongly affects their evolution and appearance.
- The state of the central object (temperature, luminosity, mass loss) will affect the local environment (envelope + disk) and thus the accretion process.
- Calculating the *coupled* evolution of envelope, disk, and central star is particularly important for high mass stars, where the interactions between the forming star and surroundings is the greatest.

Description of Cases calculated

1. Evolutionary tracks of non-accreting protostars: Comparison tracks from "birthline" to end of hydrogen burning were calculated with stellar evolution code.
2. Evolution of accreting (proto-) stars at given accretion rates: 2a. Accretion at a given constant rate was assumed (Figs 1-2): 10^{-5}, 10^{-4}, 10^{-3}, and 10^{-2} $M_\odot$ yr^{-1}. 2b. Accretion at prescribed variable rate was assumed (Figs. 3-4).
3. Hybrid calculation (evolution of central protostar coupled with 2D radiation hydrodynamics of 10 $M_\odot$ collapsing core (redo case F of YB99): Accretion rate onto the central star is determined by the flow of gas into the central "sink" cell of the collapse calculation (Figs. 5-8).

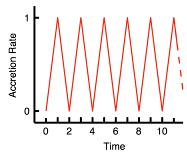

The Numerical Code: A Hybrid of two Codes

The radiation hydrodynamics code

- Explicit hydrodynamics adapted from Yorke & Bodenheimer (1999) but with improved spatial resolution: 8 "nested grids" of 80x80 grid points [8*80x80] in R- and Z- directions
- Axial symmetry is assumed; no explicit treatment of magnetic fields; angular momentum transport within disk according to α-formulism
- Radiation transfer is treated in the "gray flux-limited diffusion" approximation solved with implicit ADIP; opacities are Planck-weighted mean opacities of dusty gas (silicates, amorphous carbon, ice-coated grains)

The stellar evolution code

- Based on code *STELLAR* distributed in book "Numerical Methods in Astrophysics: An Introduction", Bodenheimer, et al. (2007)
- Spherical symmetry and hydrostatic equilibrium assumed; implicit Henyey method used; detailed equation of state
- Grey atmosphere ~1000 grid points + 200-3000 interior cells, added or subtracted as needed
- Mixing-length treatment of convection; "gray" diffusion approximation; detailed Rosseland opacities, including electron heat conduction

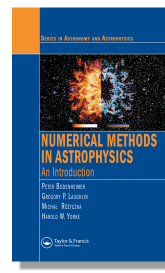

Meshing the two codes

- Material flowing into central "sink" cell is added to mass of "inner cell accretion disk" M_{ID} at the rate given by the RHD code
- Mass of central hydrostatic object for *STELLAR* is increased at rate $M_{ID}/[10^{11}$ s] and the mass of the inner cell accretion disk M_{ID} is decreased accordingly

1. Non-accreting Protostars

Calculated tracks of non-accreting protostars are shown in Figures 1, 3 and 6 for comparison to cases with accretion

2. Accreting (Proto-)Stars

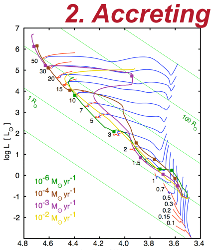

Figure 1. Evolution of intrinsic core luminosity vs. effective temperature for stars accreting at the constant rates as indicated. Non-accreting pre-main sequence tracks (blue) and main sequence (red) evolutionary tracks are shown for comparison. Filled squares denote positions at which 0.3, 1, 3, 10, 30 and 100 $M_\odot$ accreted .

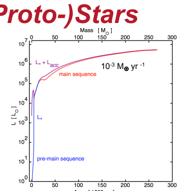

Figure 2. Evolution of intrinsic core luminosity and accretion luminosity for a constant accretion rate of 10^{-3} $M_\odot yr^{-1}$ (see Fig. 1)

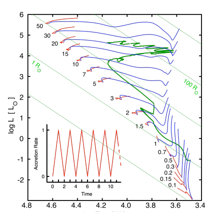

Figure 3. Evolution of intrinsic core luminosity vs. effective temperature for an accretion rate which varies from 0 to 10^{-3} $M_\odot yr^{-1}$ back to 0 every 2000 yr. (see Fig. 4)

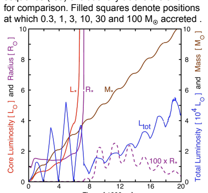

Figure 4. Time evolution of intrinsic core radius R_* , mass M_* and luminosity L_* vs. time for an accretion rate which varies from 0 to 10^{-3} $M_\odot$ yr^{-1} back to 0 every 2000 yr (see Fig. 3 inset). The total luminosity L_{tot} (sum of core luminosity and accretion luminosity) is shown on a different scale.

Discussion and Conclusions

The pre-main sequence phase of star formation can **not** be expected to follow the evolutionary tracks that we have learned about in school: evolution along the "Hayashi" tracks as a fully convective constant-mass star, followed by the "radiative" contraction to the main sequence. Accretion onto the star will play a prominent role in the evolution during these early phases.

Recently, Yorke & Bodenheimer (2008) and Hosokawa & Omukai (2008) employed stellar evolution codes to study the evolution of accreting stars at *specified* high accretion rates. In spite of differences in the codes used and the outer boundary conditions, both pairs of authors found that accretion at high rates cause the stars to bloat up during certain phases, sometimes exceeding 100 solar radii (BY08; see also Figs. 3 and 4 with maximum stellar radii ~250 $R_\odot$). The fact that stellar radii remain small for low mass objects even while they accrete material at a high rate, implies that accretion luminosity will dominate the stellar emission during these early phases (see Figs. 4 & 5).

The calculations presented here demonstrate that the stellar evolution code *STELLAR* can be incorporated into hydro-codes and calculations of collapse.

Yorke & Bodenheimer (1999) discuss the evolution of collapsing, density-peaked ($\rho \propto r^{-2}$) molecular cores, taking into account angular momentum transport in the accretion disks that form. The central source located within the central grid cell was treated approximately; BY99 estimated both the intrinsic luminosity of the protostar and its radius (important for calculating the accretion luminosity). The redo of their case F shows that high accretion rates *do* occur (see Fig. 5). Although the density, temperature and velocity structure of the accreting envelope and disk as shown in Fig. 8 looks similar to the corresponding diagrams of BY99, there are sometimes significant differences in the evolution of the luminosity and radii of the central protostars.

Due to the high rate of binarity among O-stars and preponderance of tight binaries with periods of the order of days (e.g. Zinnecker & Yorke 2007), the concept of bloating during the accretion phase is an important aspect of high mass star formation. Expansion to large radii greatly increases the cross section for stellar collisions and near collisions. Mass transfer between close binaries may occur − in extreme cases resulting in a common envelope of the binaries. Episodes of common envelope evolution will result in tighter binaries or even coalescence of the binaries. Finally, the accretion process from the disk onto the star can be strongly enhanced by the sudden radius growth of the star as the inner parts of the disk are enveloped.

3. Case F Results (10 $M_\odot$)

case	M $M_\odot$	R_{80} AU	R_1 AU	Ω 10^{-13} s^{-1}	T_{out} K	E_T/E_G	E_R/E_G	t_{ff} yr
F	10	6667	0.68	2.0	100	0.39	0.0033	30,700

M total mass of collapsing cloud; $\mathbf{R_{80}}$ outer cloud radius; $\mathbf{R_1}$ size of central cell; **Ω** initial rotation rate; $\mathbf{T_{out}}$ outer temperature; $\mathbf{E_T/E_G}$ initial ratio thermal to gravitational energy; $\mathbf{E_R/E_G}$ initial ratio of rotational to gravitational energy; $\mathbf{t_{ff}}$ initial free-fall time The initial density distribution was: $\rho \propto r^{-2}$

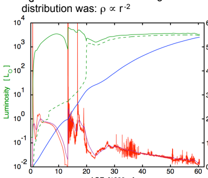

Figure 5. Evolution of luminosity, stellar mass and mass growth rate. The dashed green line shows the core luminosity; the solid green line includes the contribution of the core's accretion shock. The purple line depicts the accretion rate onto the hyrdrostatic core, whereas the red line is the accretion rate into the innermost cell.

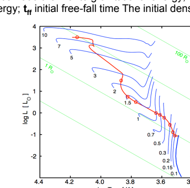

Figure 6. Evolution of intrinsic core luminosity vs. effective temperature (red) for case F compared to non-accreting pre-main sequence (blue) and main sequence (red) evolutionary tracks. Circles denote positions at which 0.15, 0.2, 0.3, 0.5, 0.7, 1, 1.5, 2, 3 and 5 $M_\odot$ accreted onto the star. Non-accreting tracks were calculated with stellar evolution code *STELLAR.*

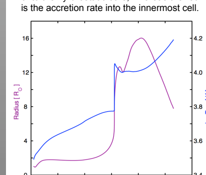

Figure 7. Evolution of stellar radius (purple) and effective temperature (blue) for case F as a function of mass accreted onto the star.

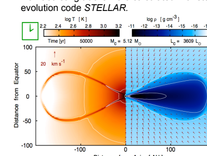

Figure 8. Temperature (left), density (right), and velocity (arrows) structure of accreting envelope + disk about 50,000 yr after onset of collapse. The central cell containing the evolving protostar shown in Figs. 5, 6 and 7 is smaller than an AU.

References

Bodenheimer, Laughlin, Rozyczka, Yorke (2007), "Numerical Methods in Astrophysics: An Introduction"
Hosokawa & Omukai (2008) ASP Conf.Ser. 387, eds. H. Beuther, H. Linz, T. Henning, p. 255
Yorke & Bodenheimer [YB99] (1999) ApJ, 525, 330
Yorke & Bodenheimer [YB08] (2008) ASP Conf.Ser. 387, eds. H. Beuther, H. Linz, T. Henning, p. 189
Zinnecker & Yorke (2007) ARAA 45, 481

Acknowledgements: This work was performed at the Jet Propulsion Laboratory, operated by the California Institute of Technology under contract to the National Aeronautics and Space Administration (NASA). HWY is partially supported by NASA under the "Origins of Solar Systems" Program.

Jet Propulsion Laboratory
California Institute of Technology
Pasadena, California

www.jpl.nasa.gov